**ORIGINAL PAPER**

# Application of UAV photogrammetry products for the exploration of dimension stone deposits: a case study of the Majestic Rose quarry, Kerman province, Iran

Hadi Shahriari[1] · Mehdi Honarmand[2] · Saeed Mirzaei[3] · Joan-Cristian Padró[4]

## Abstract

This research aims to show the capability of unmanned aerial vehicles (UAVs) for aerial fracturing survey, determining the block size, and estimating the reserve of dimension stone deposits. The Majestic Rose marble quarry in Kerman province, Iran, was selected as the case study. The quarry presents large outcrops and rugged topography. UAV-based imagery was applied as a time- and cost-effective solution for acquiring highly accurate geological and structural data across the deposit. An aerial survey was conducted at 70 m altitude with 70% lateral and 80% front image overlaps. About 47 ground control points (GCPs) were used to increase the surveying accuracy. The orthophoto image with a spatial resolution of 2.97 cm/pix was applied to specify geological units and the deposit boundary. Due to the importance of fractures in the exploitability of dimension stones, the orthophoto image and hill-shade model were used for enhancing the fractures. A fracture density map was created to delineate critical zones. The fracture spacing was determined to estimate the average block size in critical zones. A digital elevation model (DEM) with an accuracy of 2.28 cm was used to reconstruct the 3D deposit model. An accurate block model was created using the 3D deposit model for estimating the resources in the eastern and western sub-zones. This research showed the capability of UAVs in increasing the efficiency of mineral exploration programs of dimension stones. The proposed methodology can be customized for other surficial deposits considering the mineralization type and geological setting.

**Keywords** UAV-based imagery · Dimension stone · Geological mapping · Aerial fracturing survey · Photogrammetry · Reserve estimation

## Introduction

Mineral exploration is a sequential procedure that comprises successive phases from regional-scale investigation to local-scale studies to discover new mineral deposits. Thanks to high coverage, remote sensing is a time- and cost-effective solution for detecting mineral potentials in a regional-scale investigation (Atif et al. 2021; Eldosouky et al. 2021; Ishagh et al. 2021; Pour et al. 2021; Yousefi et al. 2021, 2022). On the local scale, commercial unmanned aerial vehicles (UAVs), also known as drones, have accomplished

✉ Hadi Shahriari
  shahriarihi@gmail.com

  Mehdi Honarmand
  mehonarmand167@gmail.com

  Saeed Mirzaei
  mirzaei_s@nicico.com

  Joan-Cristian Padró
  JoanCristian.Padro@uab.cat

[1] Department of Mining Engineering, Vali-e-Asr University of Rafsanjan, Rafsanjan, Iran

[2] Department of Ecology, Institute of Science and High Technology and Environmental Sciences, Graduate University of Advanced Technology, Kerman, Iran

[3] Department of Mining Engineering, Sarcheshmeh Copper Mine, National Iranian Copper Industries Co. (NICICo), Rafsanjan, Iran

[4] Departament de Geografia, Universitat Autònoma de Barcelona, Edifici B, Bellaterra, Spain

high-resolution geophysical, geological, and mineral mapping at reasonable prices (Szentpeteri et al. 2016; Kirsch et al. 2018; Carabassa et al. 2019; Ren et al. 2019; Park and Choi 2020; Shahmoradi et al. 2020; Fotheringham and Paudyal 2021). UAV-based imagery is at the beginning of its path toward playing a more influential role in the mining industry, from mineral exploration to mine reclamation (Park and Choi 2020; Shahmoradi et al. 2020).

Today, UAVs are looking forward to making more contributions to mineral exploration campaigns because of their ability to carry geophysical, multispectral, and hyperspectral sensors (Szentpeteri et al. 2016; Parvar et al. 2017; Ostad-Ali-Askari et al. 2017; Kirsch et al. 2018; Carabassa et al. 2019; Ren et al. 2019; Shahmoradi et al. 2020; Heincke et al. 2019; Golian et al. 2020; Honarmand and Shahriari 2021). UAVs have filled the gap of remotely sensed data below the height flight of common airborne and heliborne platforms. The literature review demonstrates the application of high-resolution photogrammetric data in geological and geophysical mapping using low-cost UAVs. Vasuki et al. (2014) prepared a map of geological faults using UAV imagery on the east coast of Tasmania, Australia. Blistan et al. (2016) carried out the documentation of rock outcrops of a surface quarry in Slovakia. Tziavou et al. (2017) performed the structural geological mapping of a fault zone outcrop using fixed-wing and multi-rotor UAVs in Scotland. Parvar et al. (2017) conducted a magnetometry survey using a multi-rotor UAV to enhance chromite-bearing host rocks in Oman. Heincke et al. (2019) used fixed-wings and multi-rotor platforms for hyperspectral imaging and magnetometry in Finland. Dai et al. (2020) utilized UAV data to locate dike swarms with the aim of gold exploration in China.

Some applications of UAVs involve data acquisition at the deposit scale to reconstruct 3D outcrop geometry. Szentpeteri et al. (2016) prepared the 3D geological model of an open-pit mine using a quadcopter in Malaysia. They described the method of creating geological models on deposit scale using UAV data. Blistan et al. (2016) applied UAV photogrammetry to create a 3D model of inaccessible rock outcrops of a quarry in Slovakia. Kirsch et al. (2018) accomplished lithological and hydrothermal alteration mapping in a gravel quarry by UAV-borne multi-sensor hyperspectral imagery in Germany. Dujoncquoy et al. (2019) used UAV photogrammetry to reconstruct 3D outcrop models for oil and gas exploration in Spain. Honarmand and Shahriari (2021) applied high-resolution geological mapping using UAV imagery to locate vein-type Cu mineralization in Iran. Padró et al. (2022) implemented a workflow for quarry restoration management based on 3D modeling of a quarry in Spain.

The ultimate aim of mineral exploration programs is to find out whether the ore deposit can be technically and economically mineable or not. The solution is provided through

a step-by-step procedure that attempts to determine critical parameters for evaluating the reserve. The literature review demonstrates that the use of UAVs on a deposit scale exploration has been limited to general applications such as the preparation of geology maps and 3D geological models (e.g., Szentpeteri et al. 2016; Kirsch et al. 2018; Ren et al. 2019; Honarmand and Shahriari 2021). The current research tries to expand the use of UAVs in mineral exploration by increasing the efficiency of operations. The Majestic Rose marble quarry in Kerman province, Iran, is selected as the case study. The large outcrops of the quarry are visible on the highlands. The quarry has rough relief and unsafe slopes preventing thorough geological and fracturing surveys. As a result, conventional techniques of fracturing surveys cannot satisfy evaluating the potential of providing commercial right-angled blocks in the Majestic Rose marble quarry. The reconstruction of an accurate 3D deposit model to accomplish the primary estimation of the resource is, thus, difficult using traditional topographic surveying methods. Accordingly, the main objectives of the research are defined as follows:

a) high-resolution fracturing survey to outline critical zones for complementary field investigation
b) estimating the average block size in critical zones using photogrammetry products for estimating the mineral resource
c) estimating the mineral resource by reconstructing an accurate block model

To achieve the research objectives, an aerial survey is performed using a low-cost, lightweight UAV. The methodology of the aerial survey is discussed in detail. The type and quality of photogrammetry products are described. Fieldwork and laboratory studies are also performed to evaluate the physical, chemical, and geomechanical specifications of the marble stone. An accurate block model is reconstructed based on photogrammetry products. Finally, resource estimation is undertaken using the block model.

## Geological setting

The study area is located in the southwestern part of the Sanandaj-Sirjan Zone (SSZ). The SSZ is one of the significant metallogenic zones of Iran (Stöcklin 1968). It is a metamorphic belt related to Zagros orogeny with the NW–SE trend (Fig. 1). The lithology includes mostly Mesozoic rocks, while Paleozoic rocks have no considerable exposures except in the southeast (Berberian 1977; Mohajjel et al. 2003). Eftekharnejad (1981) defined two subdivisions, north SSZ and south SSZ, separated in the Golpaygan area. The south SSZ was deformed in the Late Cretaceous and intruded by many
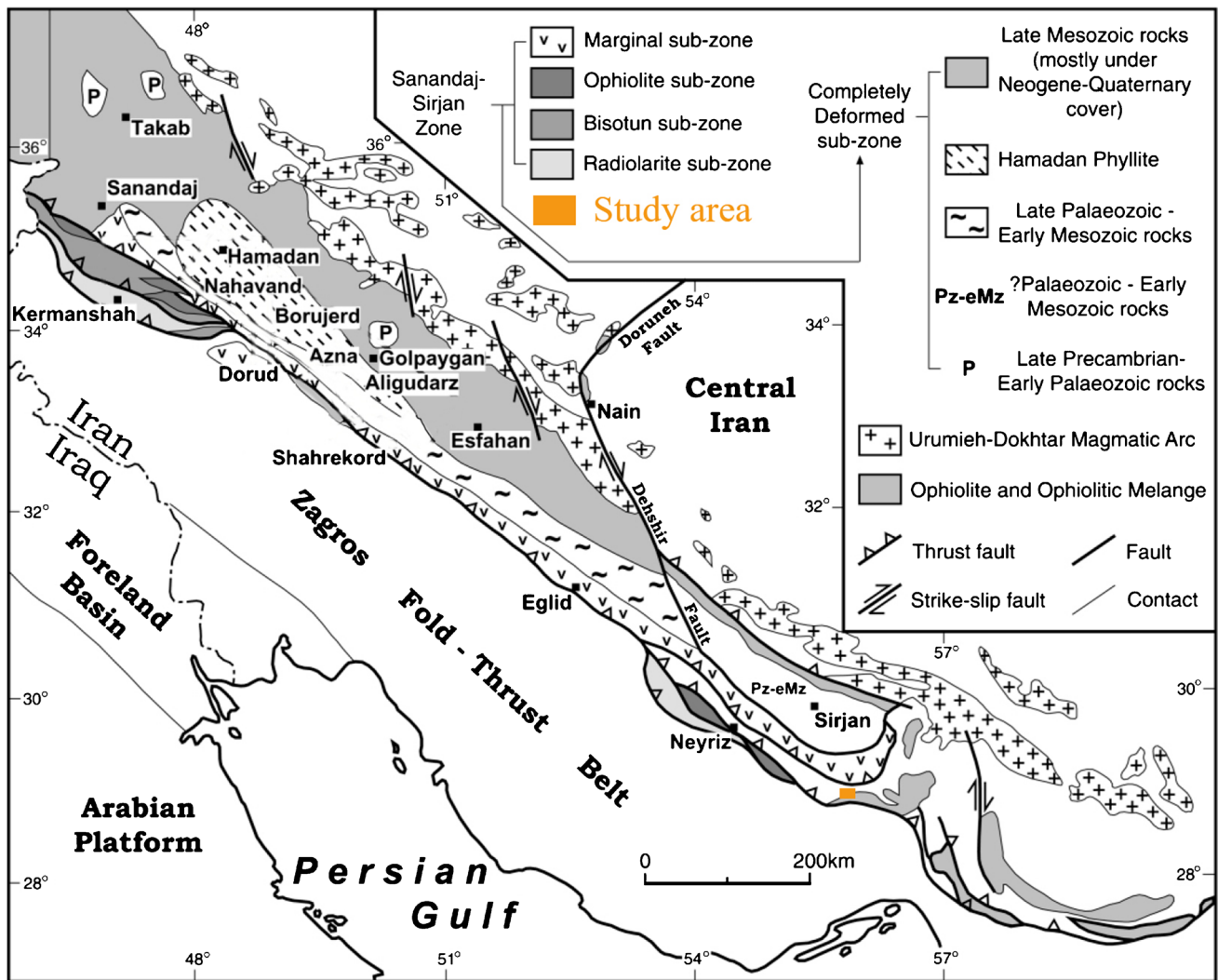
**Fig. 1** Simplified tectonic map of southeastern Iran, including the Sanandaj-Sirjan Zone (Mohajjel et al. 2003)

felsic intrusive rocks. Rock deformation and metamorphism happened during the Middle to Late Triassic in the south SSZ (Eftekharnejad 1981; Ghasemi and Talbot 2006). In the south SSZ, after volcanic activities in the Late Jurassic to Early Cretaceous, continental red beds were deposited and covered by Lower to Middle Cretaceous carbonate rocks (Stöcklin 1968; Berberian and King 1981; Ghasemi and Talbot 2006). After that, the SSZ was affected by an intense deformation until the end of the Cretaceous.

Mohajjel et al. (2003) divided the SSZ into five parts from NW to the SE, including complexly deformed, marginal, ophiolite, Bisotun, and radiolarite sub-zones (Fig. 1). Based on Fig. 1, the Majestic Rose quarry is situated in the radiolarite sub-zone. This sub-zone was composed of Triassic–Cretaceous limestone and dominant radiolarite. Figure 2 shows the northwestern of the Orzuieh geology map (GSI 1996). Based on the Orzuieh geology map, thin to medium

bedded limestone, sandy and silty clay flat, and alluvial deposits are dominant geological units in the study area.

## Materials and methods

Dimension stone is a natural rock used for ornamental or decorative purposes (Ashmole and Motloung 2008). The quality and exploitability of dimension stones are expressed in terms of appearance (color and texture), discontinuities, intrusives, alterations, contact zones, inclusions, and accessory minerals (Reddy 2002; Ashmole and Motloung, 2008). The exploration activities thus include geological and structural mapping, geophysical studies, and core drilling to resolve the quality and exploitability concerns (Ashmole and Motloung 2008). Conducting comprehensive research requires easy and safe access to all deposit parts
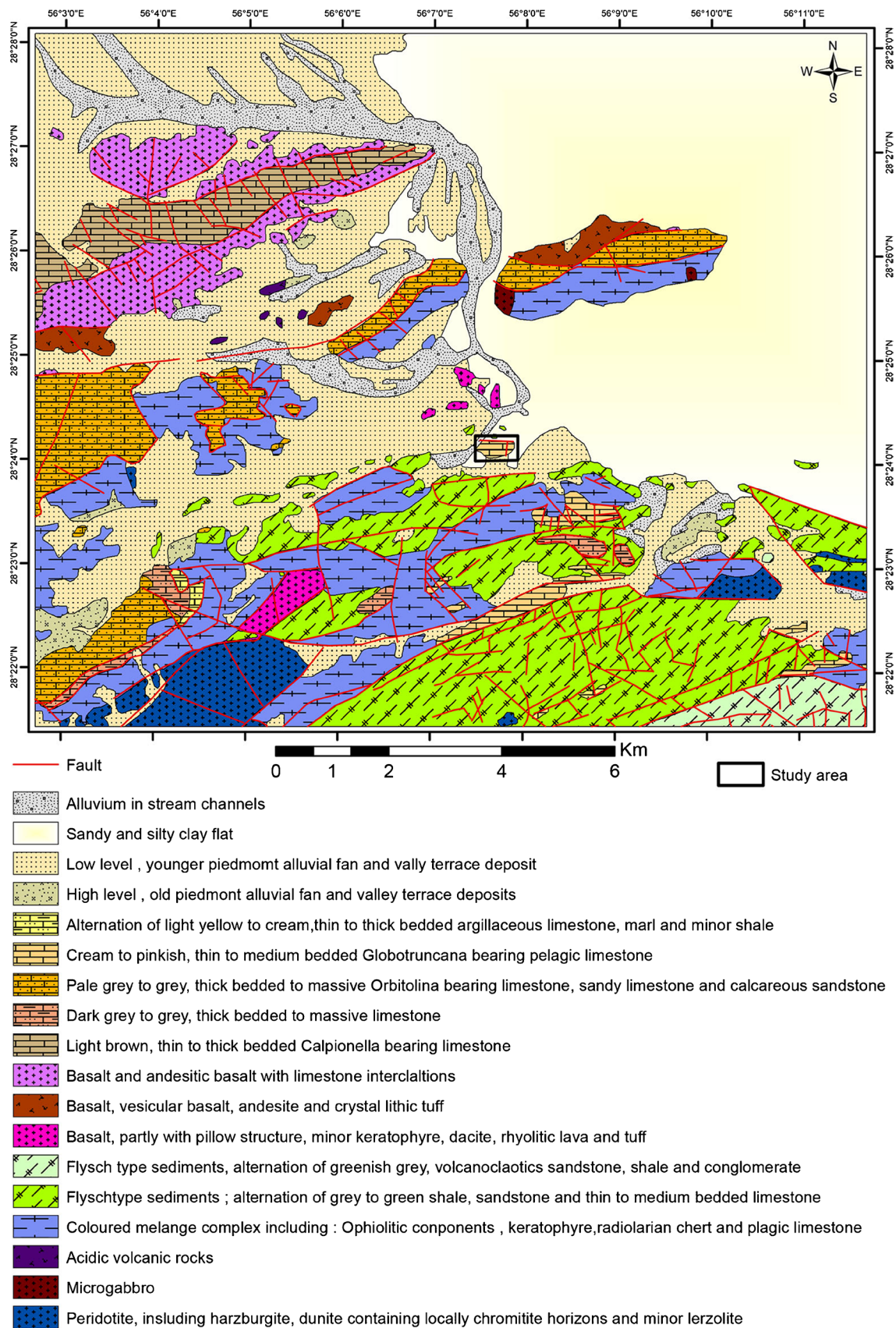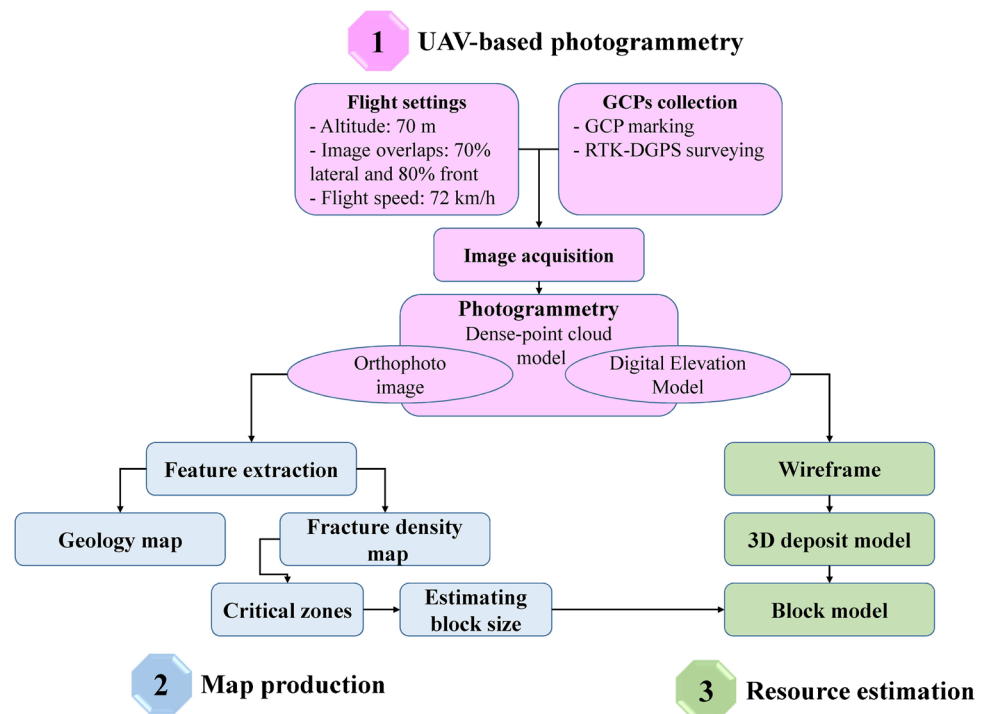
**Fig. 2** Regional geology map of the study area (GSI 1996)

Legend:

— Fault

Alluvium in stream channels

Sandy and silty clay flat

Low level, younger piedmomt alluvial fan and vally terrace deposit

High level, old piedmont alluvial fan and valley terrace deposits

Alternation of light yellow to cream, thin to thick bedded argillaceous limestone, marl and minor shale

Cream to pinkish, thin to medium bedded Globotruncana bearing pelagic limestone

Pale grey to grey, thick bedded to massive Orbitolina bearing limestone, sandy limestone and calcareous sandstone

Dark grey to grey, thick bedded to massive limestone

Light brown, thin to thick bedded Calpionella bearing limestone

Basalt and andesitic basalt with limestone interclaltions

Basalt, vesicular basalt, andesite and crystal lithic tuff

Basalt, partly with pillow structure, minor keratophyre, dacite, rhyolitic lava and tuff

Flysch type sediments, alternation of greenish grey, volcanoclaotics sandstone, shale and conglomerate

Flyschtype sediments; alternation of grey to green shale, sandstone and thin to medium bedded limestone

Coloured melange complex including: Ophiolitic conponents, keratophyre, radiolarian chert and plagic limestone

Acidic volcanic rocks

Microgabbro

Peridotite, insluding harzburgite, dunite containing locally chromitite horizons and minor lerzolite

Study area

**Fig. 3** Workflow of the research



to develop the fieldwork. The Majestic Rose marble quarry displays large and extended outcrops on rough topography that make it challenging to perform fieldwork and terrestrial surveying. Hence, complete coverage was promised through aerial mapping. A UAV-based survey was conducted to collect high-resolution data across the deposit. This research involves three sections. The first section was dedicated to aerial survey and photogrammetry. The flight setting is performed in DJIGo software, and acquired images are geometrically corrected using a collection of ground control points (GCPs). Photogrammetric processing is done using Agisoft PhotoScan v1.4.4 software. In the second section, geological features such as boundaries of geological units and structural features such as faults are derived in ArcGIS 10.8 software. Geology and fracture density maps are produced in this stage. The geology map is used to determine the boundary of the quarry. The critical zones are identified by the fracture density map. In the last section, an accurate 3D deposit model is reconstructed in Agisoft PhotoScan software and the resource is estimated by creating the block model in Datamine Studio RM software. Figure 3 shows the research workflow and presents how the photogrammetry products are used in different parts of the exploration program.

## Platform and sensor specification

Some of the DJI Phantom platforms have been successfully utilized in geological studies (Blistan et al. 2016; Szentpeteri et al. 2016; Kirsch et al. 2018; Dai et al. 2020; Dujoncquoy

et al. 2019; Honarmand and Shahriari 2021). In this research, aerial imagery was undertaken using a DJI Phantom 4 Pro V2.0. This quad-rotor UAV acquires high-resolution images using a built-in CMOS camera. The camera is mounted on a 3-axis (roll, pitch, yaw) stabilized gimbal. The technical parameters of the UAV are given in Table 1.

## Flight setting and acquisition plan

The acquisition plan in UAV-based photogrammetry missions can include platform-sensor system settings, flight path design, marking and surveying GCPs, and capturing the images. Proper setting of the platform-sensor system is performed based on the required spatial resolution. Image quality is a function of sensor specification, the type of UAV, and flying height. The spatial resolution of images affects the quality and quantity of data extraction (Stöcker et al. 2018). Flight altitude directly affects the quality of the acquired images and subsequent photogrammetry products (Tziavou et al. 2017). Lowering the flight altitude improves the spatial resolution to derive more information from images, but increases the operating cost (Tziavou et al. 2017; Dai et al. 2020). Dai et al. (2020) examined different altitudes to evaluate the impact of flying height on the operational cost and spatial resolution using a DJI Phantom 4 Pro. Flight tests were performed at 10, 25, 50, and 200 m altitudes. They mentioned the accuracy and efficiency of geological mapping at an altitude of 50 m for key areas. Honarmand and Shahriari (2021) achieved a spatial resolution of 3.26 cm/pix by imaging at an altitude of 70 m

**Table 1** Technical specification of DJI Phantom 4 Pro V2.0 (https://www.dji.com/phantom-4-pro-v2/specs)

| | | |
|---|---|---|
| Platform | Weight (including battery and propeller) | 1375 g |
| | Diagonal size (without propeller) | 350 mm |
| | Max. airspeed | S mode: 72 km/h (sport mode) |
| | Max. angle of inclination | S mode: 42° |
| | Max flight time | About 30 min |
| | Operating temperature | 0 to 40 °C |
| | Positioning | GPS/GLONASS |
| Camera | Sensor | 1-inch CMOS<br>Effective pixels: 20 megapixels |
| | Lens | Field of view 84° 8.8 mm/24 mm (35 mm format equivalent) f/2.8, autofocus from 1 m to ∞ |
| | Max. image size | 3:2 aspect ratio: 5472×3648<br>4:3 aspect ratio: 4864×3648<br>16:9 aspect ratio: 5472×3078 |
| | Mechanical shutter speed | 8–1/2000s |
| | Electronic shutter speed | 8–1/8000 s |

using a DJI Phantom 4 Pro V2.0. They accomplished geological and structural mapping in a vein-type Cu porphyry deposit. In this research, a spatial resolution of less than 5 cm was promised to increase the accuracy of geological and structural mapping. To achieve the proposed resolution, the flight was performed at a height of 70 m based on previous experiences (Dai et al. 2020; Honarmand and Shahriari 2021).

The application of calibration targets, such as bar targets, slanted edge tests, and Siemens star targets, is essential for measuring the spatial resolution of UAVs. The Siemens star target takes on a circular shape that makes it possible to measure the spatial resolution in all directions for the flight path (Orych 2015). Depending on the scale of the study, sinusoidal and binary (discrete) patterns are chosen for laboratory and outdoor purposes, respectively (Loebich et al. 2007; Honkavaara et al. 2008; Orych 2015). In this research, a binary (discrete) Siemens star target on a flat surface was performed to measure the spatial resolution of

the CMOS camera (Fig. 4a) (Honkavaara et al. 2008; Orych 2015; Honarmand and Shahriari 2021).

Flight path planning is required to achieve the promised accuracy. Accuracy is one of the main quality metrics that is employed to assess the geospatial data (Stöcker et al. 2018). Image overlap is one of the main parameters that control the accuracy of aerial surveying. In the case of non-RTK (real-time kinematic) UAVs, the accuracy is often improved using GCPs. Therefore, it is essential to consider a GCP network when using non-RTK UAVs. GCPs are marked and surveyed before the flight. In addition, several checkpoints are needed to measure the overall accuracy of the operation. These checkpoints are distributed between GCPs. Appropriate image overlap combined with the grid of GCPs can meet the desired accuracy (Szentpeteri et al. 2016).

The built-in GPS of DJI Phantom 4 Pro V2.0 is only used for establishing a geo-tagged image for general applications. So, it cannot satisfy the accuracy requirement for local-scale mapping in geology and mining applications. In this study,

**Fig. 4** **a** Siemens star target and **b** SOUTH Galaxy G1 + receiver on a benchmark
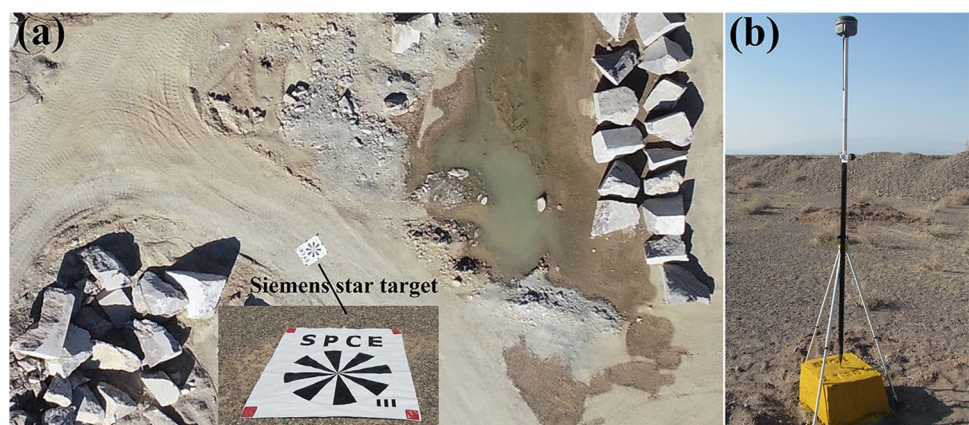
an accuracy of less than 5 cm was aimed for photogrammetry products. The flight path was designed in DJIGo software, considering lateral and forward overlaps of 70% and 80%, respectively. More than 45 temporary GCPs were marked in the study area. A pair of SOUTH Galaxy G1 + receivers were used to measure the exact location of GCPs based on a ground-based real-time kinematic-differential global positioning system (RTK-DGPS) (Fig. 4b). Also, six checkpoints with known coordinates were used for calculating the overall accuracy.

## Photogrammetry procedure and products

The procedure of photogrammetric processing and producing different 2D and 3D products is presented in Fig. 5. The photogrammetric processing was performed using Agisoft PhotoScan v1.4.4 software. The acquired images and camera positions were used to establish the spares-point cloud model. The model was built by finding the matched points of overlapping images and estimating the camera location for each image. GCPs were used for optimizing the camera positions and indirect georeferencing of the spares-point cloud model to create the dense-point cloud model (Padró et al. 2019; Honarmand and Shahriari 2021). The dense-point cloud model was utilized to generate the mesh model and derive the digital elevation model (DEM). Based on Fig. 5, the orthophoto (orthomosaic) image was created using the mesh model.

Geology maps with different scales are prepared as an essential part of any exploration program. They are the basis of developing the fieldwork and estimating the resource. Thanks to the high resolution, the orthophoto image was applied for preparing the geology map (Fig. 5). Accordingly, the orthophoto image was digitized to outline the boundary of geological units using ArcGIS 10.8 software. To complete

the geology map, the rock types were assigned to geological units after conducting the geological survey.

The homogeneity of dimension stone deposits is a challenging issue in reserve evaluation and mine design. The homogeneity can be stated in terms of color, texture, and discontinuities (Ashmole and Motloung 2008). The block size of dimension stone deposits is estimated based on the situation and spacing of fractures. Depending on the project objectives, fracture surveys can be performed using various destructive and non-destructive methods (Fig. 6). Although destructive methods are expensive and time-consuming, they assist in collecting data for sophisticated modeling of fractures in large projects (Jalalian et al. 2021). Among non-destructive methods, non-contact surveying approaches such as aerial photogrammetry can satisfy surveying fractures with low cost and high speed even in inaccessible areas (Yarahmadi et al. 2015; Jalalian et al. 2021).

In rough terrains, conducting a fracturing survey is a difficult task and cannot yield complete coverage using terrestrial approaches. The aerial photogrammetric survey provides appropriate coverage and enables mapping the fractures, even in inaccessible localities (Elkarmoty et al. 2017; Jalalian et al. 2021). Honarmand and Shahriari (2021) recommended the application of orthophoto image and hillshade model for enhancing structural lineaments. The hillshade model was established using the orthophoto image in ArcGIS software (Fig. 5). The orthophoto image and hillshade model were used for digitizing fractures. A density map of the fractures was created to delineate the zones with high fracture intensity in ArcGIS software.

The 3D model of deposits is gradually developed during the exploration activities to estimate the reserve. Due to the high accuracy, photogrammetry products can be used for reconstructing the 3D deposit model. Appropriate image overlap combined with a grid of GCPs ensures obtaining the
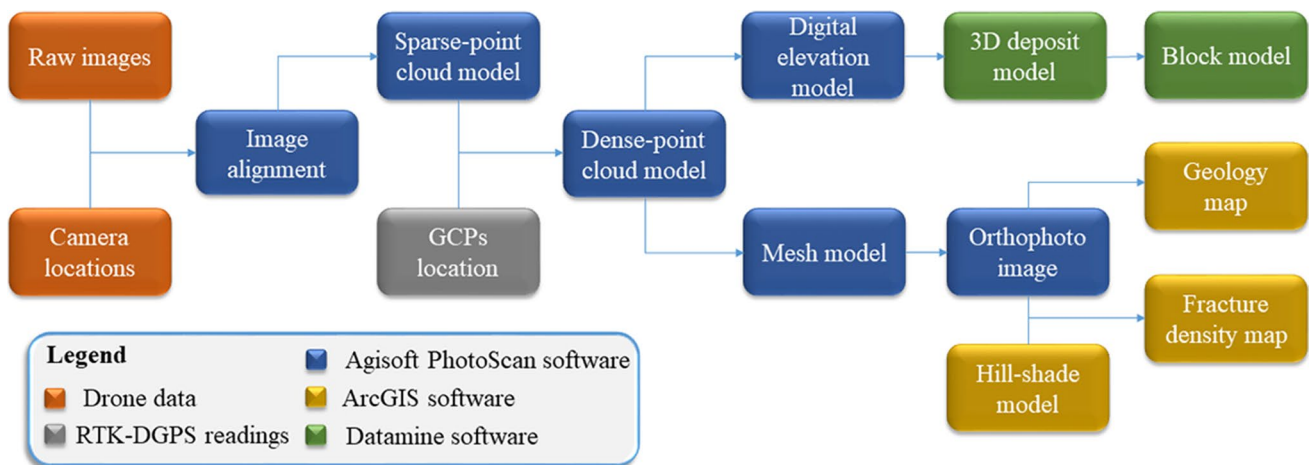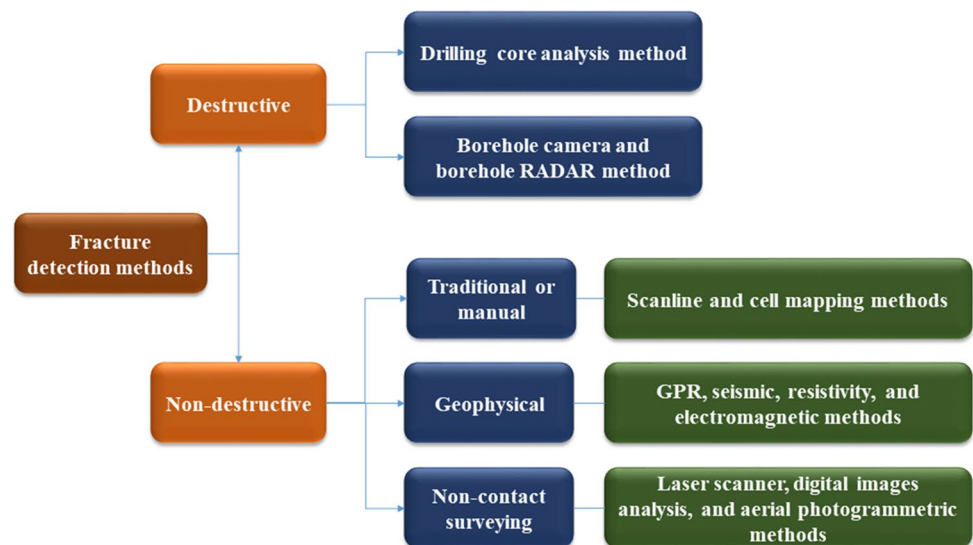


**Fig. 5** Workflow of photogrammetric processing

**Fig. 6** Classification of fracture detection methods (Elkarmoty et al. [2017])



promised accuracy. Based on Fig. 5, the DEM of the Majestic Rose quarry was imported to the Datamine software to build the wireframe of the deposit. The deposit boundary and large fractures were imported as vector files and modeled in the wireframe. Finally, a block model was created in Datamine software to estimate the source.

### Fieldwork and laboratory studies

The geological survey and laboratory studies were considered to complete the geology map and determine the specification of the marble stone in the study area. Several representative samples were collected to define mineralogical, physical, geomechanical, and chemical specifications. The chemical durability tests indicated that the stone could be damaged by acidic solutions (e.g., HCl) while it was durable against basic solutions (e.g., NaOH). The stone showed an effective porosity of 0.4–0.5, which is classified as a very low porous stone (Siegesmund and Dürrast [2011]). The freezing and thawing test (10 cycles of freezing and thawing in ± 20 °C) presented the fair resistance of the stone against the changes in temperature due to the low water absorption capacity. Geomechanical properties were determined using uniaxial compressive strength (UCS), Brazilian tensile strength (BTS), and point-load strength index (PLSI)

**Table 2** Rock mechanics specifications of marble in the Majestic Rose quarry

| Test type | Core length to diameter | Load direction to the lamination | |
|---|---|---|---|
| | | Parallel | Vertical |
| UCS (MPa) | 2.5 | 46 | 43.5 |
| BTS (MPa) | 0.5 | $4.65 \pm 0.68$ | $3.06 \pm 0.39$ |
| PLSI (MPa) | 1.0 | $3.23 \pm 0.34$ | $3.91 \pm 0.19$ |

(Table 2). Based on UCS, BTS, and PLSI tests, the marble stone was classified as a medium-strength rock.

## Results

### Geological mapping

The Majestic Rose marble quarry is divided into area 1 and area 2 (Fig. 7). Area 1 is under exploitation using the diamond wire cutting method in two working benches. Area 2 was in the early stages of an exploration project. The UAV-based imaging was performed and the resulting orthophoto image was used for constructing the geology map.

Based on the acquisition plan, aerial imagery was performed at a flying altitude of 70 m. As a result, a spatial resolution of 2.97 cm/pix was calculated for the orthophoto image. This resolution specified the boundary of geological units and the trace of fractures on the orthophoto image in ArcGIS software. Figure 8 shows the geology map of the study area after conducting the geological survey and laboratory studies.

During the fieldwork, several samples were collected to evaluate the color variation and appearance of the marble stone, as well as discriminating rock types for completing the geology map. The Majestic Rose stone is often a brown marble with white veins (Fig. 9a). The mineralogy was investigated through thin sections and XRD analysis. Calcite, dolomite, and quartz veins were embedded in a micritic matrix (Fig. 9b). A slight lamination was observed in some thin sections due to low-grade metamorphism. Based on XRD analysis, calcite is the major phase, while quartz and albite are minor phases. XRF results are provided in Table 3. $SiO_2$ and CaO are the principal oxides, and $Fe_2O_3$ varies between 0.51 and 3.47%.

**Fig. 7** Mesh model of the Majestic Rose marble quarry
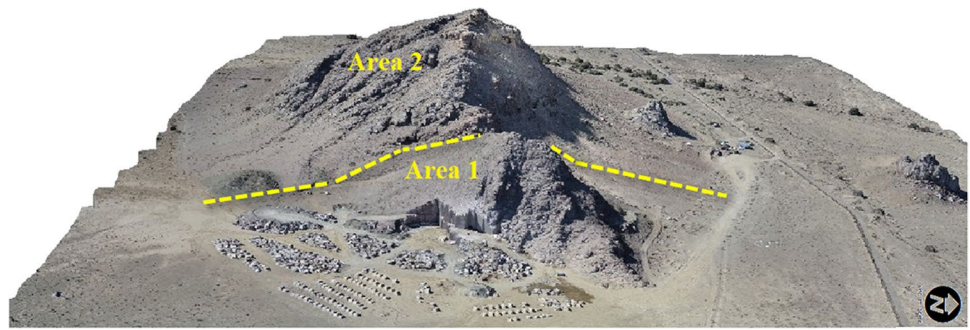


## Aerial fracturing survey

The potential of extracting right-angled blocks in commercial size is a critical issue for evaluating the dimension stone quarries. A fracturing survey is, thus, undertaken to reveal the structural defects and determine the geometry of rock blocks in dimension stone quarries. Due to the rough topography of the study area, UAV-based photogrammetry was considered for the fracturing survey. High-resolution photogrammetry products were used to determine the orientation, spacing, and density of the fractures before applying field surveying methods. Although fracture detection was performed using the orthophoto image, the hill-shade model assisted in extracting the fractures. Figure 10a displays the enhanced fractures in the study area. The study of fractures focused on two issues, areas with high fracture intensity (critical zones) and block size determination in critical areas. To specify critical zones, a fracture density map was prepared in the ArcGIS software. Accordingly, two critical zones were delineated in the south and east of area 2 (Fig. 10b). These critical zones should be evaluated using the geophysical methods (e.g., ground-penetrating radar) in the next stage. The strike of fractures is presented in Fig. 10c.
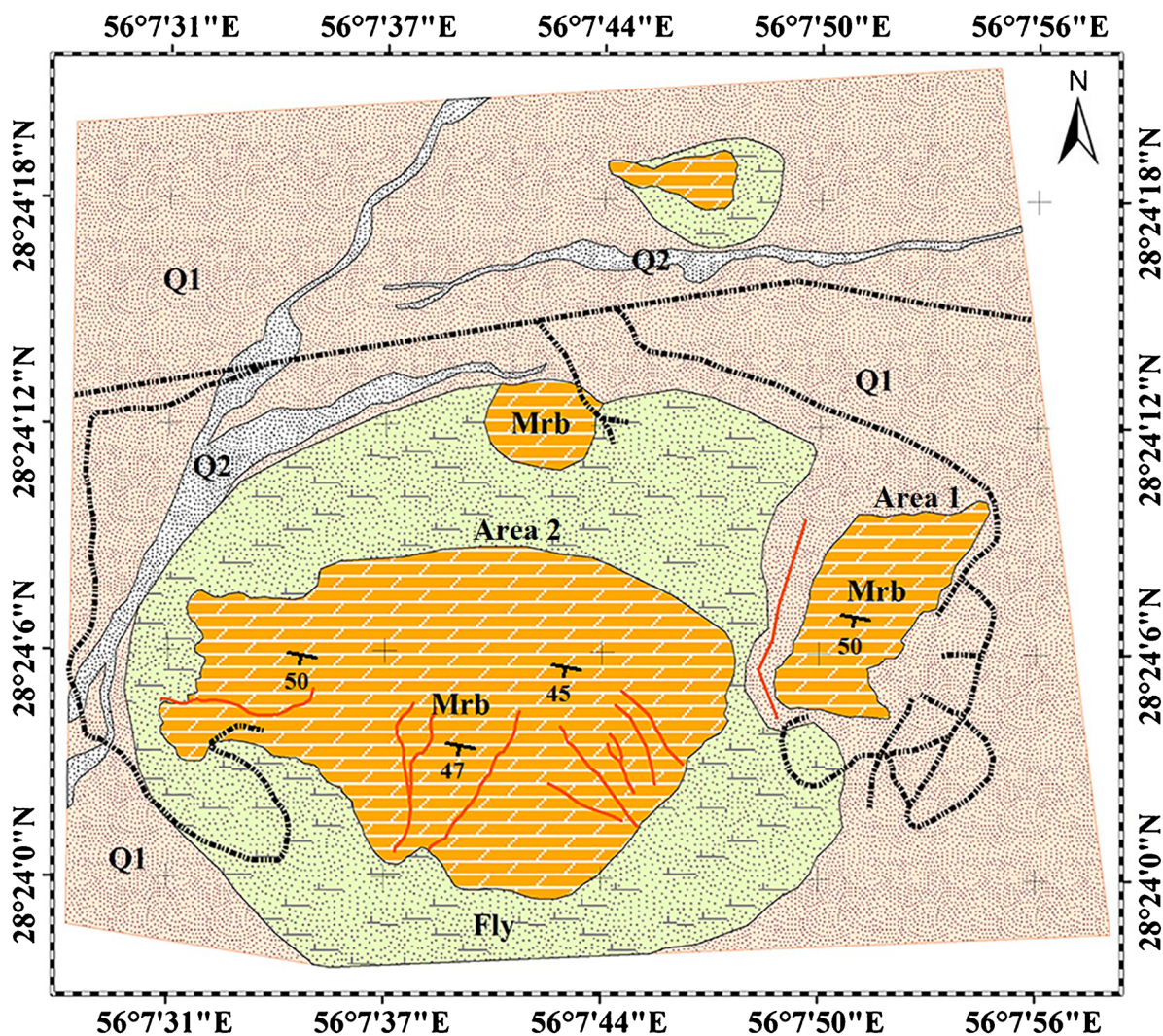
## 3D deposit model

Photogrammetry products have accomplished reconstructing accurate 3D models for geology and mining application (Dujoncquoy et al. 2019; Dai et al. 2020). The accuracy of 3D models is influenced by image overlap and can be improved by using GCPs. By applying 70% lateral and 80% forward overlaps, about 1245 images were captured in a 0.56 km$^2$ area. In Fig. 11a, the blue color indicates perfect image overlap. This level of coverage was supported by 47 GCPs to achieve an accuracy better than 5 cm. Figure 11b displays the locations of 47 GCPs and six checkpoints. The root mean square errors (RMSE) of 2.28 cm and 3.21 cm were calculated for GCPs and checkpoints, respectively (Table 4).

To reconstruct the 3D deposit model, a wireframe was established based on the deposit DEM in the Datamine software. The deposit boundary and structural features were modeled in the wireframe to create the 3D deposit model (Fig. 12).

## Discussion

The exploration plan for dimension stone deposits includes several sequences such as the desktop study, field mapping, detailed mapping, geo-radar survey, core drilling, reserve evaluation, quarry testing, and test processing (Luodes et al. 2002). Ashmole and Motloung (2008) offered another layout with some changes such as desktop study, field evaluation, detailed mapping, drilling, geophysics, bulk sampling, and quarry testing. In this research, UAV imagery was conducted just after the desktop study to supply data for the next steps in the Majestic Rose marble quarry. Geological-structural mapping, geophysical exploration, and generating 3D models of mineral deposits have been typical applications of UAV-based photogrammetry in mineral exploration activities (e.g., Szentpeteri et al. 2016; Parvar et al. 2017, Kirsch et al. 2018; Ren et al. 2019; Shahmoradi et al. 2020, Honarmand and Shahriari 2021). UAV-based photogrammetry has enough potential to be applied in the other sections of mineral exploration programs, such as aerial fracturing survey and resource estimation, as demonstrated in the Majestic Rose marble quarry. The Majestic Rose marble quarry is divided into area 1 and area 2 (Figs. 6 and 8). Area 1 is under exploitation using the diamond wire cutting method in two working benches. Area 2 was in the early stages of an exploration project. UAV-based imaging was performed in the study area to develop exploration activity in area 2. The potential of extracting right-angled blocks in commercial size is a critical issue for evaluating the dimension stone quarries. A fracturing survey is, thus, undertaken to reveal the structural defects and determine the geometry of rock blocks in dimension stone quarries. The geometry of rock blocks is used for investigating the feasibility studies of dimension stone quarries (Sousa 2010; Saliu and Idowu 2014; Yarahmadi et al. 2015). Aerial photogrammetric methods can provide information about the spacing and

**Fig. 8** Geology map of the Majestic Rose marble quarry

orientation of fractures at the surface. The orientation of fractures must be defined before determining the fracture spacing. UAV-based photogrammetry at the Majestic Rose marble quarry aimed to provide complete coverage, especially for performing high-resolution fracturing surveys even in inaccessible areas. The situation of fractures is displayed in Fig. 10a. The fracture density map of Fig. 10b helps to enhance critical zones in area 2. Measuring the fracture

spacing in critical zones was used to specify the average block size. Before estimating the average block size, it is necessary to investigate the specification of fractures using the aerial data. Although a fault has separated area 1 from area 2, comparing rose diagrams in the two areas indicates similarity. Based on the rose diagrams of Fig. 10c, the dominant fracture set in area 1 and area 2 exhibits N5E orientation. Another fracture set with N75W orientation was observed in the rose

**Fig. 9** **a** Hand specimen of the marble stone, and **b** thin section in PPL mode
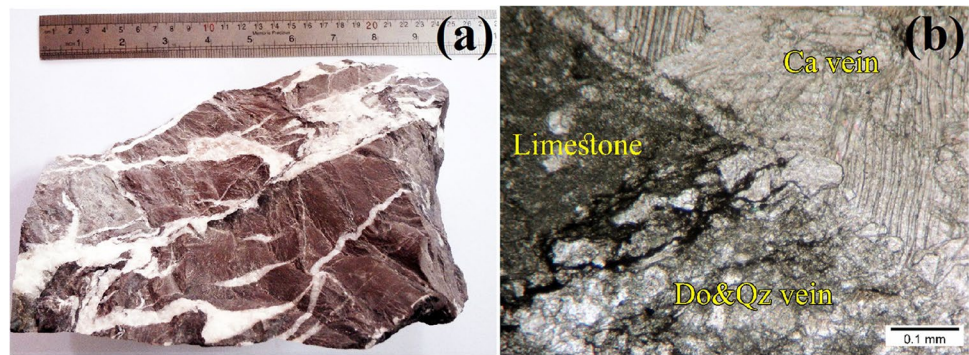


**Table 3** XRF results of rock samples in the Majestic Rose marble quarry (values are in percent and the detection limit is 0.01)

| Sample | L.O.I | $SiO_2$ | $Al_2O_3$ | BaO | $K_2O$ | CaO | $Na_2O$ | $Fe_2O_3$ | MgO | MnO | $SO_3$ | $P_2O_5$ | $Cr_2O_3$ | $TiO_2$ |
|---|---|---|---|---|---|---|---|---|---|---|---|---|---|---|
| 1 | 30.83 | 25.76 | 1.39 | <0.01 | 0.22 | 40.31 | 0.48 | 0.51 | 0.30 | 0.06 | 0.05 | 0.03 | 0.01 | 0.05 |
| 2 | 22.76 | 40.54 | 2.97 | 0.14 | 0.19 | 28.91 | 1.20 | 1.91 | 0.89 | 0.11 | 0.15 | 0.09 | 0.01 | 0.13 |
| 3 | 29.81 | 16.20 | 5.17 | <0.01 | 1.11 | 41.15 | 0.95 | 3.47 | 1.92 | 0.08 | 0.02 | 0.02 | 0.01 | 0.09 |

*L.O.I*, loss on ignition.

diagram of area 2 (Fig. 10c). Fracture spacing was calculated along several profiles perpendicular to the orientation of fracture sets in critical zones of area 2 (Fig. 10a). Accordingly, the average spacing was calculated about 8.38 m along EW strike and 9.42 m along NS strike that yielded the average block size in area 2. The experience of mining in area 1 could be used in predicting the behavior of fractures in area 2. Figure 13a shows a halved commercial block in area 1. The commercial block in the Majestic Rose marble quarry had a cross section of 6*6 m that was smaller than the measured cross section of 9.42*8.38 m in critical zones of area 2.

Field investigation ensured the results of the aerial fracturing survey. Joints were mainly filled with calcite or calcite + quartz minerals across the deposit (Fig. 9). Based on the mining experience in area 1, the joint fillings have reinforced the rock mass to increase the potential of producing healthy right-angled blocks (Fig. 13a). Figure 13b displays the situation of fractures in the quarry face of area 1. Based on Fig. 13a b, only large fractures may continue to deeper levels and show more potential to defect the marble stone compared to joints. Therefore, the results of the aerial fracturing survey were reliable for investigating the status of fractures and estimate the block size in the study area.

Evaluating the mineral deposits is a challenging duty that attempts to answer ambiguities about the quantity and quality of the reserve. The quantity parameter refers to the volume or tonnage of valuable ore minerals in the deposit. The quality of dimension stones is generally defined according to visual (e.g., color and texture) and physical

(e.g., fracture intensity) variables (Kapageridis and Albanopoulos 2016). Thus, evaluating the reserve requires a comprehensive study of color variation, the situation of joints and fractures, and some physical, chemical, and geomechanical parameters. Quality parameters can estimate the resource using geostatistical techniques (Exadaktylos and Saratsis 2020). Evaluating the resource relies on establishing an accurate 3D model of the mineral deposit. The UAV-based photogrammetry in the Majestic Rose marble quarry provided the opportunity to establish an accurate 3D deposit model at the beginning of the exploration project at a low cost. An overall accuracy of 3 cm was obtained, which is similar to the result achieved by Honarmand and Shahriari (2021) with the same platform-sensor settings. Figure 12 displays the 3D deposit model of the Majestic Rose marble quarry. The model can be gradually developed during the exploratory works in the future. The resource calculation in the Datamine software needed to define the block size to establish a block model. According to Figs. 10c and 13, the fracture characteristics are similar in the two areas, and the average block size in area 2 is larger than the commercial block size in area 1. Thus, the commercial block size of $8.0 \times 6.0 \times 6.0$ m was considered to create the block model of the deposit (Fig. 12). Consequently, the volume of resources in areas 1 and 2 was measured at about 39,000 and 2,400,000 $m^3$, respectively. The 3D deposit model is accurate enough to be developed during future exploration activities to be used in the reserve estimation stage.
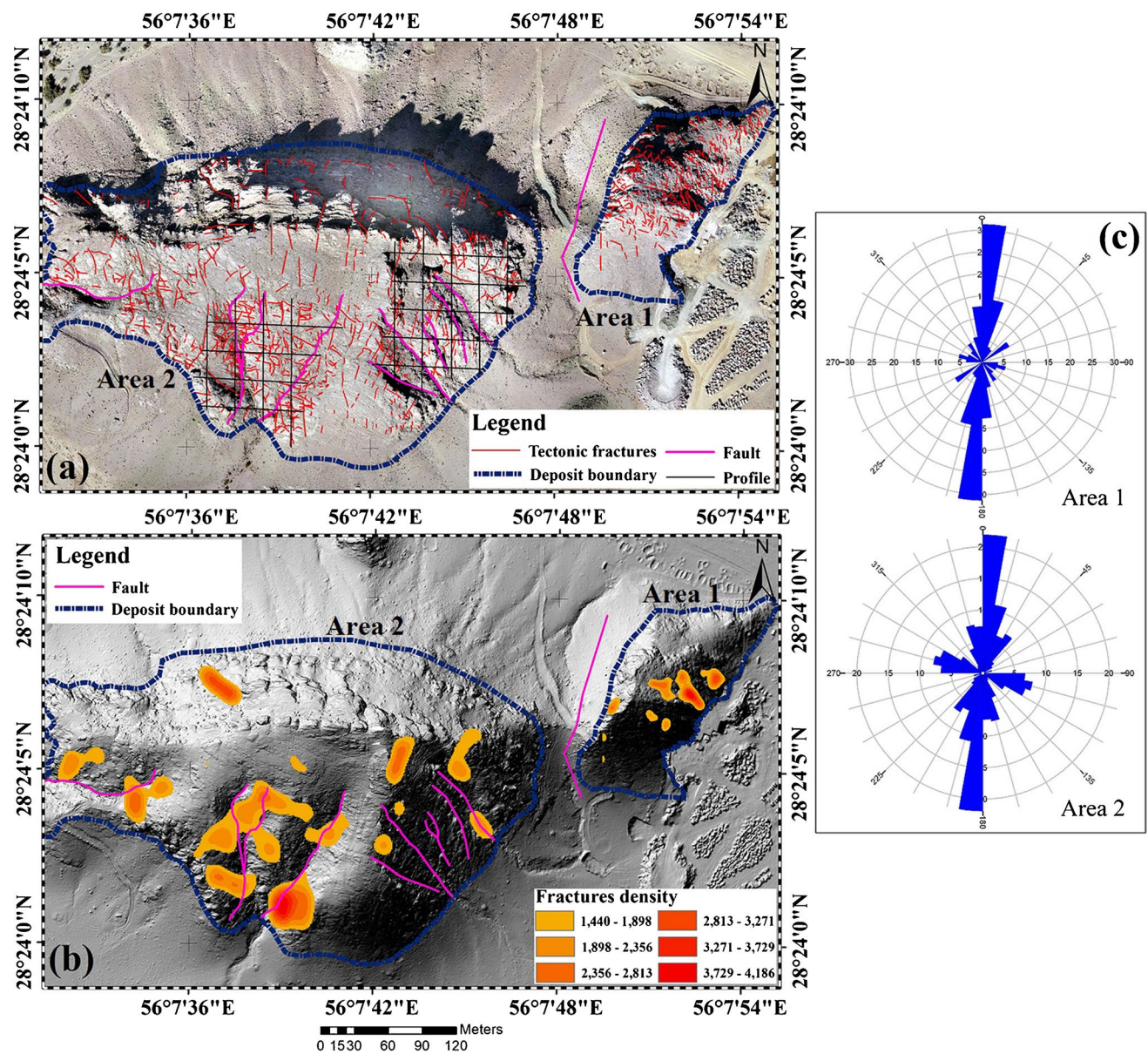
**Fig. 10** **a** Enhanced fractures using orthophoto image and hill-shade model (presented on the orthophoto image), **b** density map of fractures (shown on the hill-shade model), and **c** rose diagram of fractures in areas 1 and 2

## Summary and conclusion

In this research, a DJI Phantom 4 Pro V2.0 with its original 20-megapixel camera was employed for aerial surveying in the Majestic Rose marble quarry. The research aimed to investigate new applications of UAVs in mineral exploration campaigns. UAV imagery helped to expand exploration works into inaccessible locations in the study area. The spatial resolution of images is a function of sensor specification and flight altitude. Based on the results, to achieve a special resolution finer than 3 cm/pix, image acquisition should be performed at an altitude of 70 m. This spatial resolution is appropriate for specifying the boundary of geological units and enhancing the fractures on the orthophoto image.
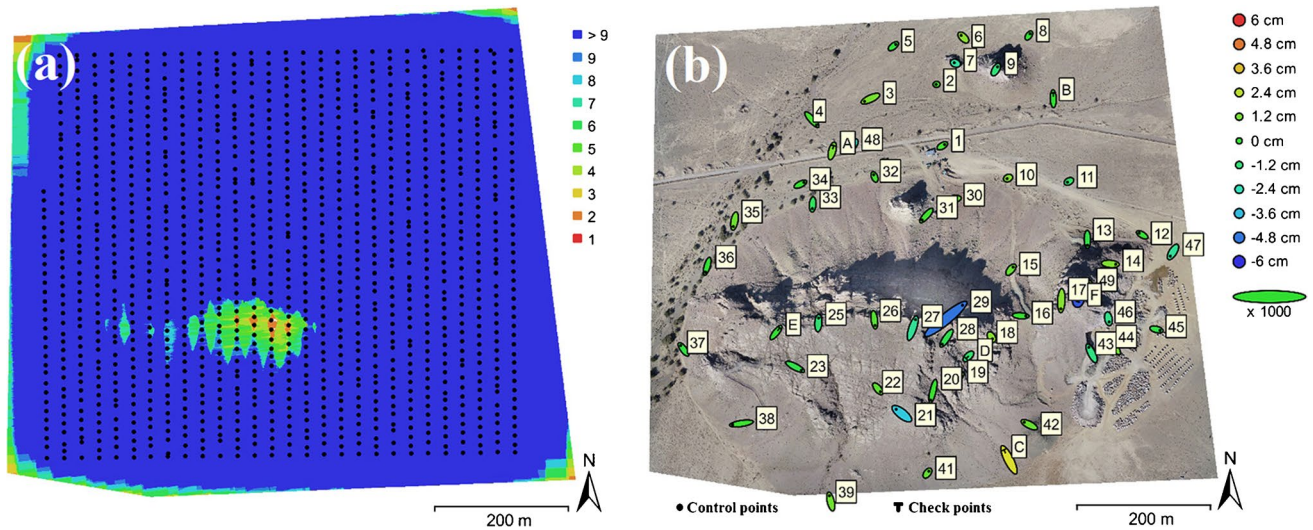
**Fig. 11** **a** Camera positions and image overlap, **b** distribution and estimated errors of GCPs and checkpoints locations (Z error is represented by ellipse color and X, Y errors are represented by ellipse shape)

**Table 4** The RMSE of GCPs and checkpoints (X—easting, Y—northing, Z—altitude)

| Point type | Count | X error (cm) | Y error (cm) | Z error (cm) | Total (cm) |
|---|---|---|---|---|---|
| GCP | 47 | 1.22 | 1.37 | 1.34 | 2.28 |
| Check points | 6 | 0.84 | 1.70 | 2.59 | 3.21 |

The study of fractures is critical for investigating the potential of extracting saleable right-angled blocks. UAV photogrammetry presented a cost-effective method to conduct fracturing surveys across the deposit in rough terrains. According to the results, the spatial resolution of about 3 cm/pix is adequate to distinguish surficial fractures through UAV-based imagery. The orthophoto image and hill-shade model are recommended for extracting structural features. The complete coverage offered by UAVs assists in preparing the fracture density map to specify critical zones. The average block size can be estimated by measuring fracture spacing in critical zones. The fracture spacing can be measured along several profiles to measure the block size. The orientation of profiles should be perpendicular to the main fracture sets. To specify appropriate places for opening the quarry, it is recommended to consider the fracture density map and large fractures.

Photogrammetry products can be used to establish an accurate 3D deposit model for estimating the reserve of surficial dimension stone quarries. The model accuracy must be ensured using proper image overlap and a network of GCPs. By considering 70% lateral and 80% front overlaps combined with a grid of GCPs, total accuracy of less than 3 cm can be obtained in a rough topography. The 3D deposit model can be created based on the deposit DEM in the early stages of exploration activity. The 3D deposit model can be divided into geological or structural sub-zones to estimate the resource. Resource estimation is done by reconstructing a block model using the average block size in critical

**Fig. 12** The 3D deposit model containing the block model of the Majestic Rose marble quarry
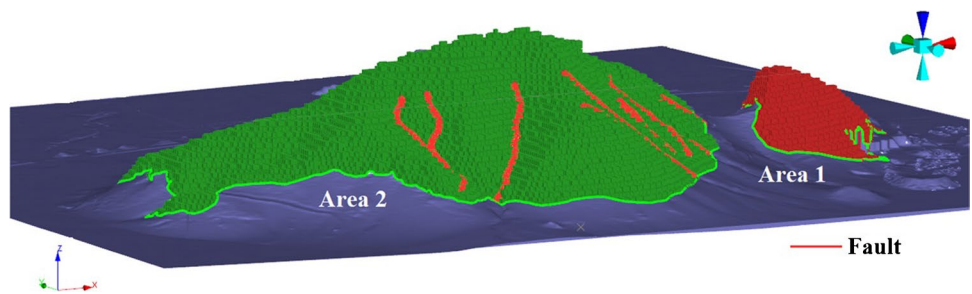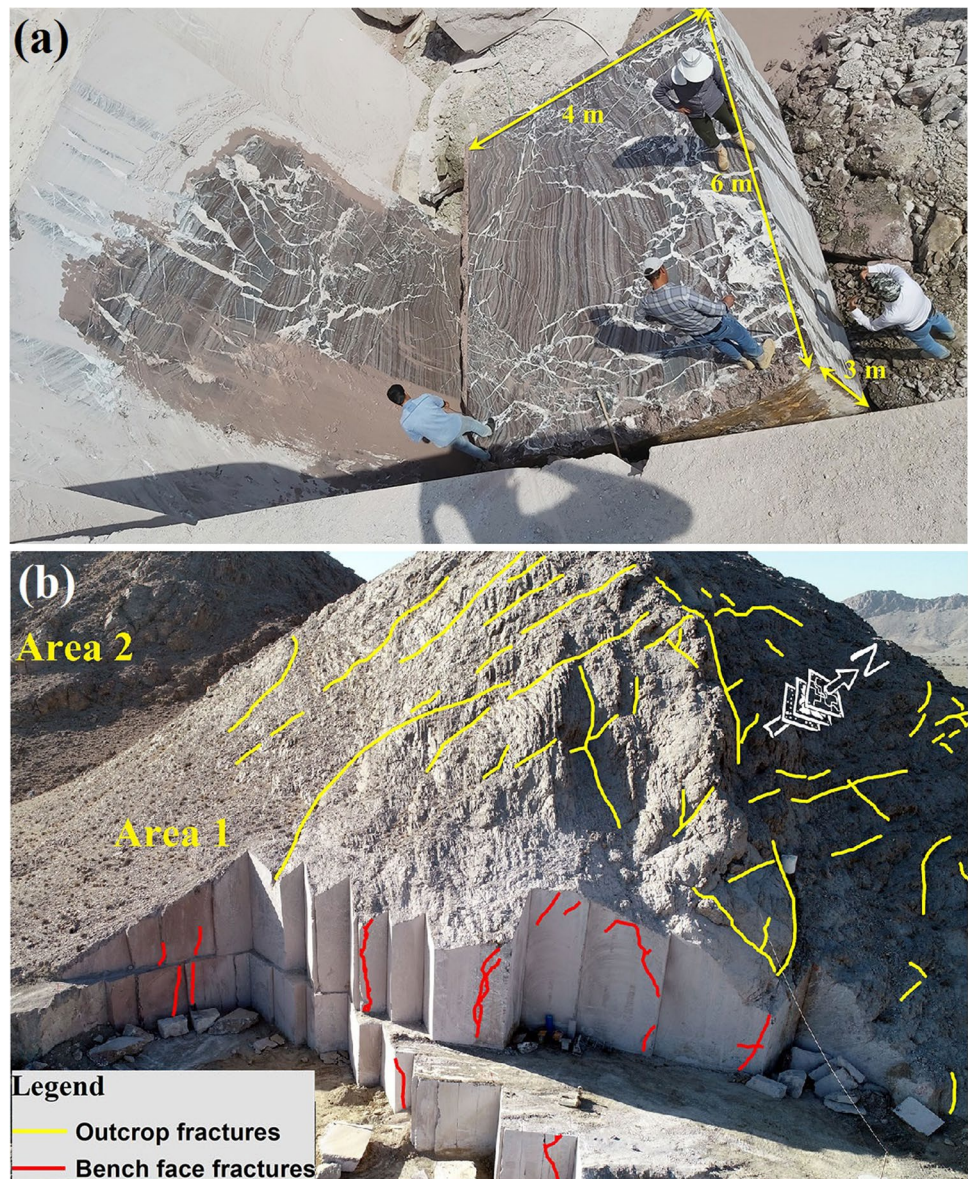
**Fig. 13** **a** A halved commercial block in the Majestic Rose marble quarry (area 1), and **b** large fractures on the quarry face in area 1



zones. This block model can be continuously updated with the progress of operations and receiving more exploration information until it is used for mine design. The layout of this research can be customized for the other surficial deposits to improve the cost-efficiency in mineral exploration campaigns. In a region with complex geology, the application of multispectral or hyperspectral sensors is recommended to provide the opportunity for mineral mapping.

## Declarations

**Ethics approval** Not applicable.

**Consent to participate** Not applicable.

**Consent for publication** Not applicable.

**Competing interests** The authors declare no competing interests.

## References

Orych A (2015) Review of methods for determining the spatial resolution of UAV sensors. International Archives of the Photogrammetry, Remote Sensing & Spatial Information Sciences, 40. https://doi.org/10.5194/isprsarchives-XL-1-W4-391-2015

Orych A (2015) Review of methods for determining the spatial resolution of UAV sensors. International Archives of the Photogrammetry, Remote Sensing & Spatial Information Sciences, 40. https://doi.org/10.5194/isprsarchives-XL-1-W4-391-2015

Ashmole I, Motloung M (2008) Dimension stone: the latest trends in exploration and production technology. In Proceedings of the Int Conference on Surface Mining 5:8

Atif Y, Soulaimani A, Ait lamqadem A, Pour AB, Pradhan B, Noua-mane EA, Abdelali K, Muslim AM, Hossain MS (2021) Identifying hydrothermally altered rocks using ASTER satellite imageries in Eastern Anti-Atlas of Morocco: a case study from Imiter silver mine. Int. J. Image Data Fusion, 1-25. https://doi.org/10.1080/19479832.2021.1958928

Berberian M, King GCP (1981) Towards a paleogeography and tectonic evolution of Iran. Can J Earth Sci 18(2):210–265

Berberian M (1977) Three phases of metamorphism in Haji-Abad quadrangle (southern extremity of the Sanandaj-Sirjan structural zone): a palaeotectonic discussion. Contribution to the seismotectonics of Iran, 239–263.

Blistan P, Kovanič Ľ, Zelizňaková V, Palková J (2016) Using UAV photogrammetry to document rock outcrops. Acta Montan. Slovaca, 21(2).

Carabassa V, Montero P, Crespo M, Padró JC, Balagué J, Alcañiz JM, Pons X (2019) UAS remote sensing products for supporting extraction management and restoration monitoring in open-pit mines. Multidisciplinary Digital Publishing Institute Proceedings 30(1):4. https://doi.org/10.3390/proceedings2019030004

Dai J, Xue L, Sang X, Li Z, Ma J, Sun H (2020) Research method for dyke swarms based on UAV remote sensing in desert areas: a case study in Beishan, Gansu, China. In IOP Conference Series: Earth and Environmental Science, 558(3), 032040. IOP Publishing.

Dujoncquoy E, Masse P, Nicol Y, Putra AS, Kenter J, Russo S, Dhont D (2019) UAV-based 3D outcrop analog models for oil and gas exploration and production. In IGARSS 2019–2019 IEEE international geoscience and remote sensing symposium (pp. 6791–6794). IEEE. https://doi.org/10.1109/IGARSS.2019.8900176.

Eftekharnejad J (1981) Tectonic division of Iran with respect to sedimentary basins. J Iranian Petroleum Society 82:19–28 (**in Farsi**)

Eldosouky AM, El-Qassas RA, Pour AB, Mohamed H, Sekandari M (2021) Integration of ASTER satellite imagery and 3D inversion of aeromagnetic data for deep mineral exploration. Adv Space Res 68(9):3641–3662. https://doi.org/10.1016/j.asr.2021.07.016

Elkarmoty, M, Colla, C, Gabrielli, E, Bonduà, S, Bruno, R (2017) A combination of GPR survey and laboratory rock tests for evaluating an ornamental stone deposit in a quarry bench. In ISRM European rock mechanics symposium-EUROCK 2017. OnePetro. 10. 1016/j. proeng. 2017. 05. 272.

Exadaktylos G, Saratsis G (2020) Methodology for the estimation and classification of white marble reserves. Min Metall Explor 37(4):981–994. https://doi.org/10.1007/s42461-020-00228-3

Fotheringham M, Paudyal DR (2021) Combining terrestrial scanned datasets with UAV point clouds for mining operations. ISPRS Ann. Photogramm Remote Sens Spatial Inf Sci 4:129–138. https://doi.org/10.5194/isprs-annals-V-4-2021-129-2021

Ghasemi A, Talbot CJ (2006) A new tectonic scenario for the Sanandaj-Sirjan Zone (Iran). J Asian Earth Sci 26(6):683–693. https://doi.org/10.1016/j.jseaes.2005.01.003

Golian M, Katibeh H, Singh VP, Ostad-Ali-Askari K, Rostami HT (2020) Prediction of tunnelling impact on flow rates of adjacent extraction water wells. Q J Eng GeolHydrogeol 53(2):236–251. https://doi.org/10.1144/qjegh2019-055

GSI (1996) Geology map of Orzuieh (Dashtvar), 1:100000. Geological Survey of Iran, Tehran

Heincke B, Jackisch R, Saartenoja A, Salmirinne H, Rapp S, Zimmermann R, ... & Middleton M (2019) Developing multi-sensor drones for geological mapping and mineral exploration: setup and first results from the MULSEDRO project. GEUS Bulletin, 43. https://doi.org/10.34194/GEUSB-201943-03-02.

Honarmand M (2021) Shahriari H (2021) Geological mapping using drone-based photogrammetry: an application for exploration of vein-type Cu mineralization. Minerals 11(6):585. https://doi.org/10.3390/min11060585

Honkavaara E, Peltoniemi J, Ahokas E, Kuittinen R, Hyyppa J, Jaakkola J, ..., Suomalainen J (2008) A permanent test field for digital photogrammetric systems. Photogramm. Eng. Remote Sens., 74(1).

Ishagh MM, Pour AB, Benali H, Idriss AM, Reyoug SAS, Muslim AM, Hossain MS (2021) Lithological and alteration mapping using Landsat 8 and ASTER satellite data in the Reguibat Shield (West African Craton), North of Mauritania: implications for uranium exploration. Arabian J Geosci 14(23):1–25. https://doi.org/10.1007/s12517-021-08846-x

Jalalian MH, Bagherpour R, Khoshouei M (2021) Wastes production in dimension stones industry: resources, factors, and solutions to reduce them. Environ Earth Sci 80(17):1–13. https://doi.org/10.1007/s12665-021-09890-2

Kapageridis I, Albanopoulos C (2016) Reserves estimation of a marble quarry using quality indicators. Bull Geological Society of Greece 50(4):1849–1858. https://doi.org/10.12681/bgsg.11924

Kirsch M, Lorenz S, Zimmermann R, Tusa L, Möckel R, Hödl P, Gloaguen R (2018) Integration of terrestrial and drone-borne hyperspectral and photogrammetric sensing methods for exploration mapping and mining monitoring. Remote Sens 10(9):1366. https://doi.org/10.3390/rs10091366

Loebich C, Wueller D, Klingen B, Jaeger A (2007) Digital camera resolution measurements using sinusoidal Siemens stars. In Digital photography III, 6502, 214–224. SPIE. https://doi.org/10.1117/12.703817.

Luodes H, Selonen O, Pääkkönen K (2000) Evaluation of dimension stone in gneissic rocks—a case history from southern Finland. Eng Geol 58(2):209–223. https://doi.org/10.1016/S0013-7952(00)00059-4

Mohajjel M, Fergusson CL, Sahandi MR (2003) Cretaceous-Tertiary convergence and continental collision, Sanandaj-Sirjan zone, western Iran. J Asian Earth Sci 21(4):397–412. https://doi.org/10.1016/S1367-9120(02)00035-4

Ostad-Ali-Askari K, Shayannejad M, Ghorbanizadeh-Kharazi H (2017) Artificial neural network for modeling nitrate pollution of groundwater in marginal area of Zayandeh-rood River, Isfahan. Iran KSCE J Civ Eng 21(1):134–140. https://doi.org/10.1007/s12205-016-0572-8

Padró JC, Muñoz FJ, Planas J, Pons X (2019) Comparison of four UAV georeferencing methods for environmental monitoring purposes focusing on the combined use with airborne and satellite remote sensing platforms. Photogramm Eng Remote Sens 75:130–140. https://doi.org/10.1016/j.jag.2018.10.018

Padró JC, Cardozo J, Montero P, Ruiz-Carulla R, Alcañiz JM, Serra D, Carabassa V (2022) Drone-based identification of erosive processes in open-pit mining restored areas. Land 11(2):212. https://doi.org/10.3390/su12062238

Park S, Choi Y (2020) Applications of unmanned aerial vehicles in mining from exploration to reclamation: a review. Minerals 10(8):663. https://doi.org/10.3390/min10080663

Parvar K, Braun A, Layton-Matthews D, Burns M (2017) UAV magnetometry for chromite exploration in the Samail ophiolite sequence. Oman J Unmanned Vehicle Systems 6(1):57–69. https://doi.org/10.1139/juvs-2017-0015

Phantom 4 Pro V2.0-Specifications–DJI. Available online: https://www.dji.com/phantom-4-pro-v2/specs.

Pour AB, Zoheir B, Pradhan B, Hashim M (2021) Multispectral and hyperspectral remote sensing data for mineral exploration and environmental monitoring of mined areas. MDPI books, 416 p. https://doi.org/10.3390/books978-3-0365-1265-5.

Reddy DV (2002) Evaluation of natural defects in commercial decorative rock deposits in Karnataka. India Gondwana Res 5(2):557–560. https://doi.org/10.1016/S1342-937X(05)70744-9

Ren H, Zhao Y, Xiao W, Hu Z (2019) A review of UAV monitoring in mining areas: current status and future perspectives.

Int J Coal Sci Technol 6(3):320–333. https://doi.org/10.1007/s40789-019-00264-5

Saliu MA, Idowu KA (2014) Investigating the effect of fracture on rock fragmentation efficiency: a case study of Kopec Granite Quarries, South Western, Nigeria.

Shahmoradi J, Talebi E, Roghanchi P, Hassanalian M (2020) A comprehensive review of applications of drone technology in the mining industry. Drones 4(3):34. https://doi.org/10.3390/drones4030034

Siegesmund S, Dürrast H (2011) Physical and mechanical properties of rocks. Stone in architecture. Springer, Berlin, Heidelberg, pp 97–225

Sousa LMO (2010) Evaluation of joints in granitic outcrops for dimension stone exploitation. Q J Eng Geol Hydrogeol 43(1):85–94. https://doi.org/10.1144/1470-9236/08-076

Stöcker C, Nex FC, Koeva MN, Zevenbergen JA (2018) Data quality assessment of UAV-based products for land tenure recording in East Africa. In NCG symposium 2018.

Stoecklin J (1968) Structural history and tectonics of Iran: a review. AAPG Bull 52(7):1229–1258. https://doi.org/10.1306/5D25C4A5-16C1-11D7-8645000102C1865D

Szentpeteri K, Setiawan T, Ismanto A (2016) Drones (UAVs) in mining and exploration. An application example: pit mapping and geological modelling. Unconventional Exploration Target & new tools in mineral and coal exploration, 45–49.

Tziavou O, Pytharouli S, Souter J (2017) The use of UAVs in engineering geological surveys: mapping along Scotland's south-west coast. In 7th international conference on engineering surveying.

Vasuki Y, Holden EJ, Kovesi P, Micklethwaite S (2014) Semi-automatic mapping of geological structures using UAV-based photogrammetric data: an image analysis approach. Comput Geosci 69:22–32. https://doi.org/10.1016/j.cageo.2014.04.012

Yarahmadi R, Bagherpour R, Sousa LM, Taherian SG (2015) How to determine the appropriate methods to identify the geometry of in situ rock blocks in dimension stones. Environ Earth Sci 74(9):6779–6790. https://doi.org/10.1007/s12665-015-4672-4

Yousefi M, Tabatabaei SH, Rikhtehgaran R, Pour AB, Pradhan B (2021) Application of Dirichlet process and support vector machine techniques for mapping alteration zones associated with porphyry copper deposit using ASTER remote sensing imagery. Minerals 11(11):1235. https://doi.org/10.3390/min11111235